Inorg. Chem. **2003**, *42*, 1532–1537

Characterization of the Low-Energy Electronic Excited States of Benzoyl-Substituted Ferrocenes

Wei Ding, Cynthia T. Sanderson, Richard C. Conover, Michael K. Johnson, I. Jonathan Amster, and Charles Kutal*

Department of Chemistry, University of Georgia, Athens, Georgia 30602

Received October 23, 2002

Resonance Raman spectroscopy has been employed to probe the excited-state distortions associated with the low-energy electronic transition of benzoylferrocene and 1,1′-dibenzoylferrocene. Resonance intensity enhancement of in-plane ligand modes, in general, and the carbonyl stretching mode, in particular, supports the proposal that the excited state populated by this transition contains appreciable metal-to-ligand charge transfer character. The redistribution of charge that occurs upon populating this state weakens the metal–ring bonding and facilitates the loss of a benzoylcyclopentadienide anion. This photochemical reaction has been investigated by an on-line electrospray ionization mass spectrometry technique that allows direct detection of primary and secondary products with solution lifetimes down to the millisecond range.

Introduction

Recent work from this laboratory[1] has confirmed earlier observations[2−4] that placing a benzoyl group on one or both cyclopentadienyl rings of ferrocene causes dramatic changes in spectral and photochemical properties. This substituent effect is clearly illustrated by the electronic absorption spectra of the representative complexes shown in Figure 1. Ferrocene (Fc) displays weak bands in the visible and near-ultraviolet regions that arise from Laporte-forbidden ligand field transitions. In contrast, benzoylferrocene (BFc) and 1,1′-dibenzoylferrocene (DFc) exhibit bands (designated 1 and 2) at longer wavelengths and with significantly higher intensities. We have proposed that these spectral differences result from the mixing of appreciable metal-to-ligand charge transfer (MLCT) character into the low-energy electronic excited states of the benzoyl-substituted complexes.[1] This MLCT contribution can be represented by a resonance structure of the type depicted in Figure 2, where the formal charges on iron and oxygen signify a shift of electron density from the metal to the ligand. Conjugation between the π orbitals of the cyclopentadienyl and phenyl rings and the adjacent carbonyl group allows the transferred charge to spread over several atoms. This delocalization of charge stabilizes the resulting excited states and lowers transition energies.[5] Moreover, the mixing of charge transfer character into the transitions relaxes the Laporte selection rule and increases band intensities.

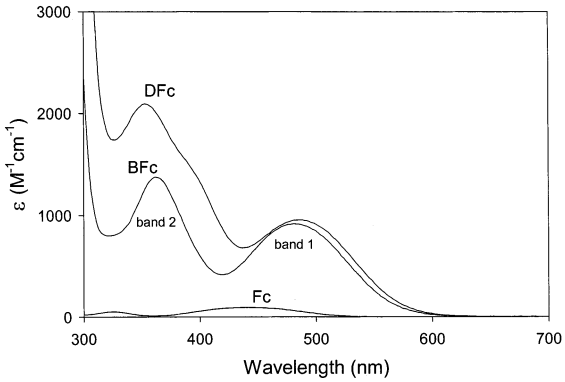

Figure 1. Electronic absorption spectra of ferrocene (Fc), benzoylferrocene (BFc), and 1,1′-dibenzoylferrocene (DFc) in room-temperature methanol.

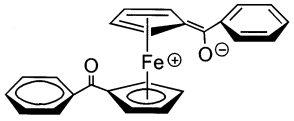

Figure 2. Resonance structure representing the MLCT character of the low-energy electronic excited states of benzoyl-substituted ferrocenes (shown here for DFc). Formal charges on atoms are circled.

* Address correspondence to this author. E-mail: ckutal@arches.uga.edu. Fax: (706) 542-9454.

(1) Yamaguchi, Y.; Kutal, C. *Inorg. Chem.* **1999**, *38*, 4861−4867.
(2) Bozak, R. E. *Adv. Photochem.* **1971**, *8*, 227−244.
(3) Tarr, A. M.; Wiles, D. M. *Can J. Chem.* **1968**, *46*, 2725−2731.
(4) Traverso, O.; Rossi, R.; Sostero, S.; Carassiti, V. *Mol. Photochem.* **1973**, *5*, 457−469.
(5) Treadway, J. A.; Loeb, B.; Lopez, R.; Anderson, P. A.; Keene, F. R.; Meyer, T. J. *Inorg. Chem.* **1996**, *35*, 2242−2246.

10.1021/ic020639z CCC: $25.00
Published on Web 02/08/2003

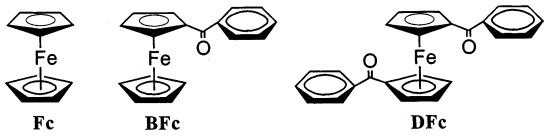

Placing a benzoyl group on one or both cyclopentadienyl rings of ferrocene also influences photochemical behavior.[1,4,6,7] While Fc is photoinert in methanol, BFc and DFc undergo reasonably efficient (quantum yield $\phi \geq 0.1$) heterolytic metal−ring bond cleavage in this solvent when irradiated with visible light (eq 1; S is solvent). We have

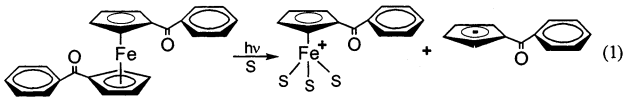

(1)

argued that this difference in photoreactivity is another consequence of mixing MLCT character into the low-energy excited states of the benzoyl-substituted ferrocenes. Examination of the resonance structure in Figure 2 reveals that this charge transfer contribution reduces the hapticity ($\eta^5 \rightarrow \eta^4$) of a cyclopentadienyl ring and enhances the susceptibility of the metal center to nucleophilic attack. The first factor weakens ring−metal bonding, while the second assists the formation of bonds to incoming ligands. Collectively, the two factors should facilitate the substitution of a benzoylcyclopentadienide anion by the surrounding solvent. From a practical standpoint, the photoreleased anion is an attractive initiating species for the polymerization of electrophilic monomers such as ethyl 2-cyanoacrylate.[8]

In this report, we describe new studies designed to test our current understanding of the electronic structures and photoreactivities of benzoyl-substituted ferrocenes. Resonance Raman (RR) spectroscopy has been employed to probe the excited-state distortions associated with the intense visible absorption band (band 1 in Figure 1) of these complexes, thereby allowing us to evaluate the proposal that this transition contains appreciable MLCT character. In addition, the chemistry that results from populating this excited state has been reinvestigated by an on-line electrospray ionization mass spectrometry (ESI-MS) technique, which has provided a more definitive characterization of photoproducts than heretofore possible.

Experimental Section

A. Materials. Benzoylferrocene (Aldrich) was sublimed under reduced pressure, while 1,1′-dibenzoylferrocene (Sigma) was recrystallized from *n*-hexane. For the ESI-MS experiments, a twice-recrystallized sample of the latter complex was purified further by column chromatography on silica gel. Excellent elemental analyses were obtained for all purified samples. Acetonitrile (Baker HPLC grade) was dried by stirring with CaH_2 (2 g/L) for 12−24 h under argon, followed by refluxing for 5 h. The solvent then was fractionally distilled, with the initial (∼15%) and final (∼30%) cuts being discarded. All other chemicals were at least of reagent-grade quality and used as received from the supplier.

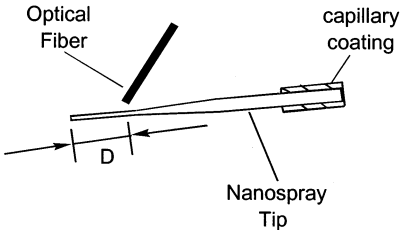

Figure 3. Schematic diagram of the nanospray tip of the ESI source. *D* defines the distance between the midpoint of the irradiated zone and the tip end.

B. Spectroscopic Methods. Raman spectra were recorded using an Instruments SA Ramanor U1000 spectrometer fitted with a cooled RCA-31034 photomultiplier tube. Spectra were recorded digitally using photon counting electronics, and improvements in signal-to-noise were achieved by signal averaging multiple scans. Absolute band positions were calibrated using the excitation frequency and CCl_4 and are accurate to ± 1 cm^{-1}. Lines from a Coherent Sabre 100 10-W argon ion laser or Coherent Innova 200-K2 krypton ion laser were used for excitation, and plasma lines were removed using a Pellin Broca prism premonochromator. Scattering was collected from the surface of the sample using 90° scattering geometry and a custom-designed sample cell,[9] which was attached to the coldfinger of an Air Products Displex model CSA-202E closed cycle refrigerator maintained at 17 K. Solid state spectra were recorded using samples prepared as KBr disks, containing 2% (w/w) K_2SO_4 as an internal standard, and the disks were attached to the surface of the sample holder using Crycon grease. Frozen solution spectra with $CHCl_3$ as the solvent were recorded using samples frozen as 15-μL droplets on the sample holder, and the solvent bands were used as an internal standard. The time course of the effect of laser exposure on Raman band intensities was monitored by optimizing alignment using a solvent or sulfate band, blocking the laser beam, adjusting the position of the sample so that the focused laser beam hits a different spot on the surface of the sample, initiating a time-based scan at fixed frequency, and then unblocking the laser beam at time zero.

ESI-MS experiments were performed in the positive ion mode on a Mariner Biospectrometry Workstation (PerSeptive Biosystems, Inc.), which combines a time-of-flight mass spectrometer with an electrospray source. Details of the instrumental setup are provided in a recent publication.[10] Figure 3 contains a diagram of the optically transparent nanospray tip, which was made from fused silica capillary tubing (100 μm i.d.). The tubing was drawn to a fine point (10−20 μm i.d. as determined by optical microscopy) at the spray-delivery end and connected at the other end to a syringe pump that delivered the sample solution at a constant flow rate. Typical operating parameters for the ESI experiments follow: spray tip potential, 1.9 kV; nozzle potential, 60 V; first skimmer potential, 11.5 V; nozzle temperature, 100 °C. The temperature in the interface region between the spray chamber and the time-of-flight mass analyzer was maintained at 100 °C to aid desolvation of electrosprayed ions. Solutions containing 1,1′-dibenzoylferrocene and a carrier cation (Na^+ or K^+ added as the iodide salt) were irradiated directly in the nanospray tip by an optical fiber that transmitted 488-nm light from an argon ion laser. The distance between the

(6) Ali, L.; Cox, A.; Kemp, T. J. *J. Chem. Soc., Dalton Trans.* **1973**, 1468−1475.
(7) Bozak, R. E.; Javaheripour, H. *Chem. Ind. (London)* **1973**, 696−697.
(8) Yamaguchi, Y.; Kutal, C. *Macromolecules* **2000**, *33*, 1152−1156.
(9) Drozdzewski, P. M.; Johnson, M. K. *Appl. Spectrosc.* **1988**, *42*, 1575−1577.
(10) Turner, C. A.; Ding, W.; Amster, I. J.; Kutal, C. *Coord. Chem. Rev.* **2002**, *229*, 9−16.

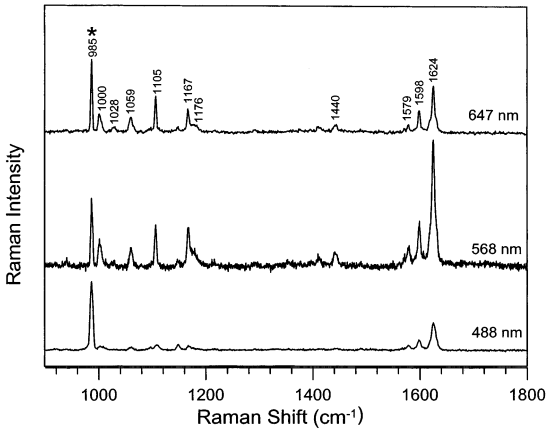

Figure 4. Solid state, low-temperature (17 K) Raman spectra of BFc obtained with 488-, 568-, and 647-nm excitations. The sample was prepared as a KBr disk containing 1.4% (w/w) BFc and 2% (w/w) K_2SO_4; the sulfate band at 985 cm^{-1} is marked with an asterisk. The spectra were collected with 150 mW of laser power at the sample, and each scan involved photon counting for 1 s every 1 cm^{-1} using 6 cm^{-1} resolution. The spectra obtained with 488-, 568-, and 647-nm excitations are the sum of 18, 10, and 50 scans, respectively.

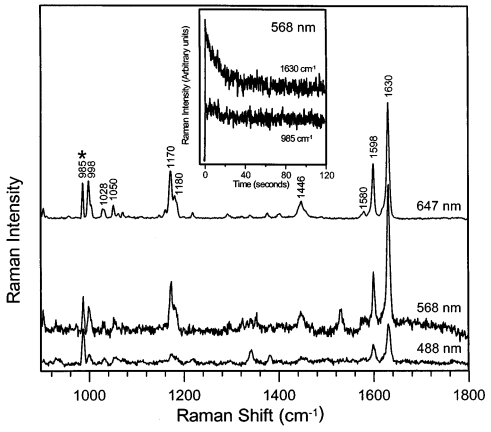

Figure 5. Solid state, low-temperature (17 K) Raman spectra of DFc obtained with 488-, 568-, and 647-nm excitations. The sample was prepared as a KBr disk containing 9.8% (w/w) DFc and 2% (w/w) K_2SO_4; the sulfate band at 985 cm^{-1} is marked with an asterisk. Measurement conditions are the same as those described in Figure 4, and the spectra obtained with 488-, 568-, and 647-nm excitations are the sum of 38, 18, and 35 scans, respectively. The inset shows a comparison of the time course of the Raman intensity measured at 985 and 1630 cm^{-1} following exposure to 568-nm laser radiation at time zero. The data were collected with a time constant of 0.01 s and an integration time of 0.01 s, using a spectral bandwidth of 5 cm^{-1} resolution and 144 mW of laser power at the sample.

midpoint of the irradiated zone and the tip end, defined as *D* in Figure 3, could be varied by adjusting the position of the fiber with a precision translation stage.

Results and Discussion

A. Resonance Raman Studies. Resonance Raman spectroscopy is well established as a powerful method for selectively enhancing the intensities of vibrational modes associated with chromophoric metal centers.[11] In addition, RR provides a means of assessing excited-state structural perturbations, since resonance enhancement is most pronounced for vibrations that mimic the distortion in the electronic excited state populated when laser radiation is tuned to the vicinity of an allowed electronic transition.[11] Charge transfer transitions are particularly effective for inducing resonant enhancement. Moreover, for complex ligands, the specific vibrational modes enhanced provide a qualitative assessment of the excited-state distortions and thereby the charge redistribution associated with the charge transfer transition. Hence, the proposal that the low-energy electronic excited states of BFc and DFc contain appreciable MLCT character can be tested by RR spectroscopy. However, the utility of this approach is limited by the extreme photolability of the benzoylcyclopentadienyl ligands in BFc and DFc, which thus far has inhibited the acquisition of high quality RR spectra for these complexes.[12] In this work, the problem of photolability has been partially alleviated by using off-resonance excitation and cooling samples to 17 K.

Raman spectra of solid state samples of BFc and DFc obtained with 647-, 568-, and 488-nm excitations are shown in Figures 4 and 5, respectively, and the Raman spectra of a frozen $CHCl_3$ solution of DFc obtained with 647- and 568-nm excitations are shown in Figure 6. In each case, the

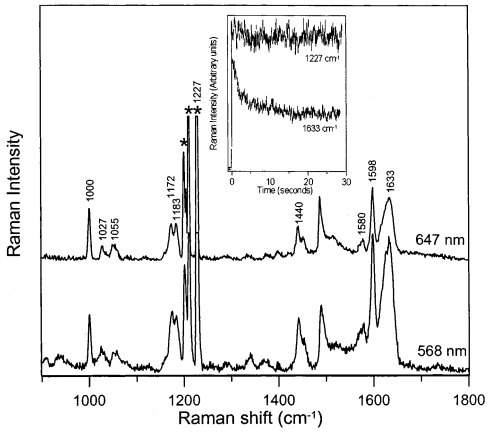

Figure 6. Low-temperature (17 K) Raman spectra of a frozen solution of 38 mM DFc in $CHCl_3$ obtained with 568- and 647-nm excitations. Solvent bands are marked with an asterisk. Measurement conditions are the same as those described in Figure 4, and the spectra obtained with 568- and 647-nm excitations are the sum of 29 and 35 scans, respectively. The inset shows a comparison of the time course of the Raman intensity measured at 1227 and 1633 cm^{-1} following exposure to 568-nm laser radiation at time zero. The data were collected with a time constant of 0.01 s and an integration time of 0.01 s, using a spectral bandwidth of 5 cm^{-1} and 210 mW of laser power at the sample.

Raman intensity has been normalized relative to a nonresonantly enhanced band of an internal standard (the 985 cm^{-1} band of K_2SO_4 in solid samples and the 1227 cm^{-1} band of $CHCl_3$ in the solution sample) in order to assess resonance enhancement and/or laser-induced photodegradation. On the basis of the literature assignments for the vibrational modes of ferrocene[13−15] and benzoic acid,[16,17] the major Raman

(11) Spiro, T. G.; Czernuszewicz, R. S. *Physical Methods in Bioinorganic Chemistry: Spectroscopy and Magnetism*; Que, L., Jr., Ed.; University Science Books: Sausalito, CA, 2000; pp 59−120.
(12) Butler, I. S.; Harvey, P. D.; Allen, G. C. *J. Raman Spectrosc.* **1987**, *18*, 1−7.
(13) Lippincott, E. R.; Nelson, R. D. *Spectrochim. Acta* **1958**, *10*, 307−314.
(14) Bailey, R. T. *Spectrochim. Acta* **1971**, *27A*, 199−202.
(15) Nakamoto, K. *Infrared and Raman Spectra of Inorganic and Coordination Compounds*, 5th ed.; John Wiley and Sons: New York, 1997.
(16) Klausberger, G.; Furić, K.; Colombo, L. *J. Raman Spectrosc.* **1977**, *6*, 277−281.

Table 1. Positions (cm^{-1}) and Assignments of the Vibrational Modes Observed in the Resonance Raman Spectra of BFc and DFc in the 900−1800 cm^{-1} Region.

	DFc		
BFc solid	solid	solution	assignment[a]
1624	1630	1633	ν(C−O)
1598	1598	1598	$\nu(C-C)_{Ph}$
1579	1580	1580	$\nu(C-C)_{Ph}$
1440	1446	1440	$\nu(C-C)_{Cp'}$
1176	1180	1183	$\delta(CCH)_{Ph}$ or $\delta(CCH)_{Cp'}$
1167	1170	1172	$\delta(CCH)_{Ph}$ or $\delta(CCH)_{Cp'}$
1105			$\nu(C-C)_{Cp}$
1059	1050	1055	$\delta(CCH)_{Cp'}$
1028	1028	1027	$\nu(C-C)_{Ph}$
1000	998	1000	$\delta(CCC)_{Ph}$

[a] Ph is phenyl; Cp and Cp′ denote unsubstituted and benzoyl-substituted cyclopentadienyl rings, respectively.

bands observed for BFc and DFc in the 900−1800 cm^{-1} region are all readily assigned to ν(C−O) and ν(C−C) stretching modes and δ(C−C−H) and δ(C−C−C) deformation modes of the benzoylcyclopentadienyl or cyclopentadienyl ligands (see Table 1).

The Raman spectra obtained for BFc in the solid state (Figure 4) demonstrate both resonance intensity enhancement of the vibrational modes of the benzoylcyclopentadienyl ligand and photodegradation of the complex using laser excitation into the low-energy absorption band centered near 470 nm (band 1 in Figure 1). The preresonance spectrum obtained with 647-nm excitation is dominated by the ν(C−O) mode of the benzoylcyclopentadienyl ligand at 1624 cm^{-1} and the ν(C−C) symmetric breathing mode of the unsubstituted cyclopentadienyl ring at 1105 cm^{-1}, and all other modes are readily attributable to internal modes of the benzoylcyclopentadienyl ligand (Table 1). The vibrational modes associated with the benzoylcyclopentadienyl ligand are selectively enhanced relative to the sulfate band at 985 cm^{-1} using 568-nm excitation into the low-energy tail of band 1. In contrast, the 1105 cm^{-1} mode of the unsubstituted cyclopentadienyl ring is not significantly enhanced, indicating that the electronic transition responsible for absorption band 1 does not involve this ring. The Raman intensities of all bands relative to the sulfate band are substantially lower using 488-nm excitation close to the absorption maximum, suggesting laser-induced photodegradation of the complex.

In accord with the analogous absorption properties in the low-energy region (Figure 1), the Raman results for DFc in the solid state (Figure 5) were found to be very similar to those observed for BFc in the solid state (Figure 4). The major differences are the absence of the ν(C−C) symmetric breathing mode of the unsubstituted cyclopentadienyl ring and no significant additional enhancement of benzoylcyclopentadienyl vibrational modes for 568-nm excitation compared to 647-nm excitation. Since the photodegradation quantum yield for DFc is 5−10 times higher than for BFc using 546-nm excitation,[1] the latter observation can be interpreted in terms of DFc being more susceptible to laser-induced photodegradation than BFc with 568-nm excitation. Moreover, direct evidence for photodegradation of DFc with 568-nm excitation was obtained by monitoring the time course of the Raman intensity of the ν(C−O) mode at 1630 cm^{-1} following exposure to the laser beam (see inset in Figure 5). Compared to the sulfate band at 985 cm^{-1}, the 1630 cm^{-1} band of DFc undergoes a substantial decrease in intensity during the first 20 s of laser exposure indicating rapid photodegradation in the solid state at 17 K.

To check the validity of the vibrational assignments and assess the extent of photodegradation in solution, we conducted parallel Raman studies for DFc in a frozen $CHCl_3$ solution at 17 K (see Figure 6). The choice of $CHCl_3$ was dictated by the need to use a solvent with Raman bands that do not overlap significantly with those of the sample. The only significant difference for the Raman spectra in solution compared to those obtained in the solid state is a substantial broadening of the ν(C═O) mode centered at 1633 cm^{-1}. This broadening is interpreted in terms of microheterogeneity in the frozen solution as a result of a low-energy barrier to rotation about the (O)C−C(Ph) bond of the benzoyl substituent.[16] Relative to the solvent bands, the vibrational modes of the benzoylcyclopentadienyl ligands exhibit significant enhancement with 568-nm excitation compared to 647-nm excitation. However, as for the solid sample, the resonance enhancement is again likely to be significantly underestimated as a result of photodegradation, since the 1633 cm^{-1} band of DFc undergoes a substantial decrease in intensity relative to the solvent band at 1227 cm^{-1} during the first 5 s of laser exposure (see inset in Figure 6).

Although the propensity for photodissociation of a benzoylcyclopentadienide anion prevents acquisition of reliable excitation profiles, the data presented in Figures 4−6 indicate that excitation into the low-energy electronic transitions of BFc and DFc leads to resonance enhancement of in-plane vibrations of the substituted cyclopentadienyl and phenyl rings in addition to strong enhancement of the carbonyl group vibration. This result is consistent with appreciable MLCT character for the low-energy transition,[18] leading to an excited state that can be depicted by the resonance structure shown in Figure 2. Changes in the C−C bond lengths in both the cyclopentadienyl and phenyl rings, as a result of enhanced conjugation between the two rings, and lengthening of the C−O bond in the excited state, would be expected to result in resonance enhancement of cyclopentadienyl ring and phenyl ring vibrations in addition to the carbonyl stretching mode. The concomitant weakening of the bonding between iron and the cyclopentadienyl ring in the excited state is, in turn, responsible for the facile photodissociation of the benzoylcyclopentadienide anion. We turn now to a discussion of this photochemical process.

B. ESI-MS Studies. Our original assignment of heterolytic metal−ring bond cleavage (eq 1) as the primary photochemi-

(17) Furić, K.; Colombo, L. *J. Raman Spectrosc.* **1986**, *15*, 23−27.

(18) A reviewer suggested the possibility that this transition may contain intraligand (IL) and/or ligand-to-ligand charge transfer (LLCT) character. We discount a significant IL contribution on the basis of the absence of band 1 in the electronic absorption spectrum of the cyclopentadienide anion (measured in AN). Likewise, we consider an LLCT contribution as unlikely, since the Raman spectra of BFc (Figure 4) show no resonance intensity enhancement of the C−C symmetric breathing mode of the unsubstituted cyclopentadienyl ring.

cal reaction of 1,1′-dibenzoylferrocene and related complexes was based upon a number of observations.[1] We found, for example, that irradiation of DFc in methanol generated a non-iron-containing product, which was identified by gas chromatography−mass spectrometry (GC-MS) as benzoylcyclopentadiene. Photolysis of DFc in acetonitrile yielded two major products detectable by ESI-MS: protonated benzoylcyclopentadiene and the cationic half-sandwich complex containing three solvent molecules. While generally supporting the occurrence of photoinduced ring loss (eq 1), these results are subject to some uncertainty arising from the analytical procedures employed. Samples were irradiated off-line and then analyzed several minutes to a few hours later by injection into the GC-MS or ESI-MS instruments. During this time interval, the primary photoproducts could have undergone secondary thermal reactions that yielded the products actually observed.

To address this concern, we have developed an on-line ESI-MS technique that minimizes the delay between the generation and analysis of photoproducts. Irradiating the sample solution flowing through the transparent nanospray tip of the ESI source (Figure 3) allows us to detect products with lifetimes in the millisecond regime. In essence, the tip functions as a photochemical reactor with an inner diameter of 10−20 μm and a length of ∼0.6 mm, the latter dimension being determined by the width of the incident light beam. The residence time of a photoproduct in solution depends on the sample flow rate and D, the distance between the midpoint of the irradiated zone and the tip end. With D = 0.84 mm, a tip inner diameter of 14 μm, and a flow rate of 40 μL/h, photoproducts require 12 ms to arrive at the tip end for spraying.

Figure 7a displays the ESI mass spectrum of an unirradiated acetonitrile solution containing DFc and Na^+ as the carrier cation. Prominent peaks appear at m/z (mass/charge) values of 417.0 and 811.1, corresponding to $(DFc-Na)^+$ and $(DFc-Na-DFc)^+$, respectively. These 1:1 and 2:1 adducts result from the Lewis acid−base interaction between the acidic sodium ion and the basic carbonyl oxygen atom of DFc. Relevant equilibria involving the various species in solution are described by eqs 2 and 3. As seen in Figure 7b, adding a large excess of Na^+ to the system shifts the equilibria in the direction that favors formation of the 1:1 over the 2:1 adduct. Confirmation of adduct stoichiometry is provided by Figure 7c, which shows that switching the carrier cation from Na^+ to K^+ causes the expected shift in m/z values of 16 units.

$$Na^+ + DFc \rightleftarrows (Na-DFc)^+ \qquad (2)$$

$$(Na-DFc)^+ + DFc \rightleftarrows (DFc-Na-DFc)^+ \qquad (3)$$

Visible-light (488 nm) irradiation of an acetonitrile (AN) solution containing DFc and Na^+ generates a rich array of photoproducts. The ESI mass spectrum shown in Figure 8 contains three major product series: (1) adducts of benzoylcyclopentadiene and a proton (m/z = 171.1) or a sodium ion (m/z = 193.0 and 363.1); (2) adducts of half-sandwich iron(II) complexes and a proton (m/z = 154.0 and 174.5);

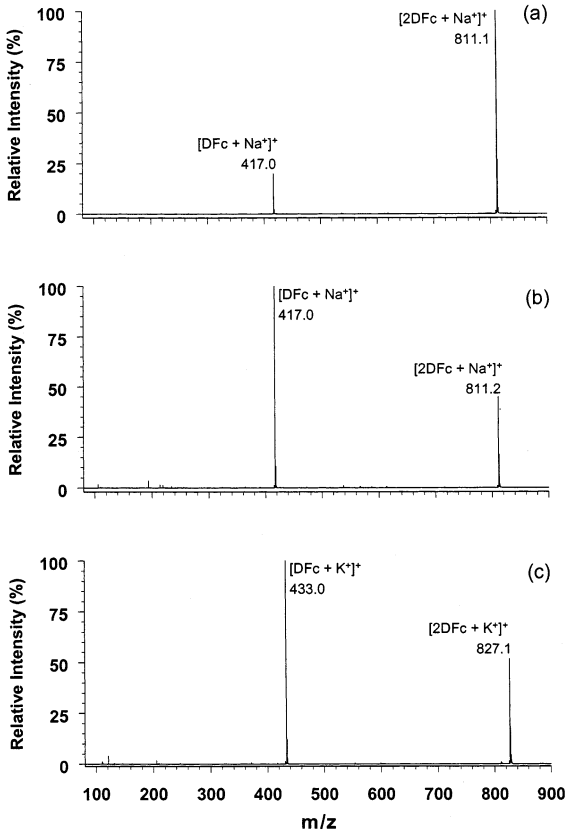

Figure 7. Electrospray ionization mass spectra of acetonitrile solutions containing DFc and a carrier cation: (a) 100 μM DFc and 160 μM Na^+, (b) 70 μM DFc and 1.4 mM Na^+, (c) 90 μM DFc and 1.2 mM K^+. Sample flow rate was 20 μL/h.

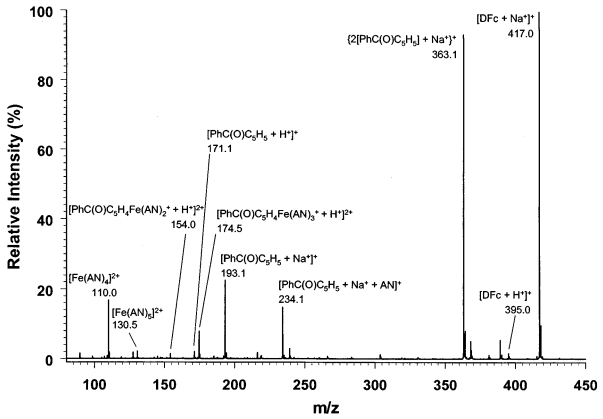

Figure 8. Electrospray ionization mass spectrum of a photolyzed acetonitrile solution originally containing 130 μM DFc and 120 μM Na^+. Laser power (488 nm) = 400 mW, D = 0.84 mm, sample flow rate = 40 μL/h.

(3) fully ring-deligated iron(II) complexes of general formula $[Fe(AN)_n]^{2+}$ (m/z = 89.5, 110.0, and 130.5 for n = 3, 4, and 5, respectively).[19] Observation of the first two product series strongly supports the assignment of heterolytic metal−ring bond cleavage (eq 1) as the primary photochemical

(19) The coordinatively unsaturated iron complexes observed within product series 2 (e.g., $[(\eta^5\text{-}C_5H_4)C(O)C_6H_5)Fe(AN)_2]^+$) and 3 (e.g., $[Fe(AN)_4]^{2+}$) result from collision-induced dissociation of acetonitrile from $[(\eta^5\text{-}C_5H_4)C(O)C_6H_5)Fe(AN)_3]^+$ and $[Fe(AN)_6]^{2+}$, respectively, after these parent species exit the ESI tip. For further information about this process, see: Ding, W.; Johnson, K. A.; Amster, I. J.; Kutal. C. *Inorg. Chem.* **2001**, *40*, 6865−6866.

reaction of DFc. The benzoylcyclopentadienide anion released in this process is sufficiently basic to abstract a proton from ambient traces of water or other protic impurities, thereby producing the neutral 1-benzoyl-1,3-cyclopentadiene molecule (eq 4).[20,21] The carbonyl oxygen atom of the benzoyl group forms Lewis acid−base adducts with a proton or a sodium ion to yield the ionic products detected by ESI-MS. Half-sandwich complexes also contain a basic carbonyl oxygen and undergo adduct formation with a proton to yield the dicationic species observed.

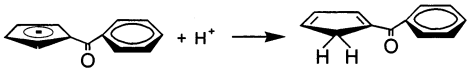

(4)

While not required by our results, it seems reasonable to suggest that photoinduced loss of the benzoylcyclopentadienide ligand occurs via one or more ring-slipped intermediates containing coordinated solvent; one possible example is the η^5,η^3-complex shown in eq 5. Such species have the option of reacting further with solvent to yield the half-sandwich complex or expelling the coordinated solvent to regenerate the parent complex. Our inability to detect ring-slipped intermediates by ESI-MS is not surprising, given their expected nanosecond lifetimes in solution.[22]

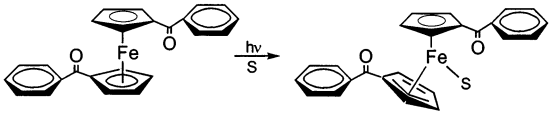

(5)

The fully ring-deligated iron(II) complexes that comprise the third photoproduct series result from the loss of the benzoylcyclopentadienide anion from the initially formed half-sandwich complex (eq 6). We suspect that this process occurs thermally, although the possibility that it results from secondary photolysis cannot be ruled out. Studies of the variation in photoproduct composition as a function of solution residence time in the ESI tip (i.e., changes in *D*) are required to resolve this issue.

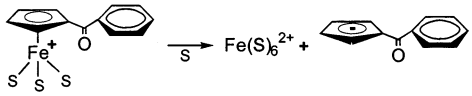

(6)

Concluding Remarks

Our resonance Raman results provide additional evidence that irradiating into absorption band 1 (Figure 1) of BFc and DFc results in the population of an excited state containing appreciable MLCT character. Accordingly, the limiting resonance structure depicted in Figure 2 offers a reasonable description of the charge distribution in this state. In a broader context, it is worth noting the close spectral resemblance between the benzoyl-substituted ferrocenes studied here and several ferrocene−(π-bridge)−acceptor complexes currently under investigation as nonlinear optical materials. For the latter family, different groups have offered alternative assignments for the absorption bands observed. Marks et al.[23] attribute the low-energy band in these complexes (comparable to band 1 in Figure 1) to a predominantly ligand field transition containing some MLCT character, while Marder et al.[24] conclude that this band arises from an MLCT transition mixed with a higher-lying π-bridge → acceptor charge transfer transition. Despite reaching different conclusions concerning the character of the transition primarily responsible for the low-energy band, both groups have recognized the importance of an MLCT contribution.

Photolyzing DFc in the nanospray tip of an ESI mass spectrometer and analyzing the products on-line has allowed us to confirm that heterolytic metal−ring bond cleavage (eq 1) is the primary photoreaction of this benzoyl-substituted ferrocene. More generally, our results underscore the value of ESI-MS for elucidating the mechanisms of photochemical reactions. This powerful technique provides mass-specific characterization of photoproducts in a single experiment, and it can detect photogenerated intermediates with lifetimes in the millisecond range. Useful information about the acid−base (eqs 2−4) and substitution (eq 6) reactions of species in solution also can be obtained. In future studies, we shall photolyze solutions containing DFc and an electrophilic monomer in the ESI tip, with the goal of obtaining information about the initiation and first few propagation steps of the ensuing anionic polymerization process.

Acknowledgment. We thank the National Science Foundation (CHE-9974579 to I.J.A. and MCB9808857 to M.K.J.) for financial support. Acknowledgment also is made to the donors of the Petroleum Research Fund, administered by the American Chemical Society, for support (to C.K.) of this research.

IC020639Z

(20) Lowry, T. H.; Richardson, K. S. *Mechanism and Theory in Organic Chemistry*; Harper and Row: New York, 1976; p 40.
(21) We confirmed the presence of 1-benzoyl-1,3-cyclopentadiene in a photolyzed sample by ^{1}H NMR spectroscopy.
(22) Dunwoody, N.; Lees, A. J. *Organometallics* **1997**, *16*, 5770−5778.
(23) Kanis, D. R.; Ratner, M. A.; Marks, T. J. *J. Am. Chem. Soc.* **1992**, *114*, 10338−10357.
(24) Barlow, S.; Bunting, H. E.; Ringham, C.; Green, J. C.; Bublitz, G. U.; Boxer, S. G.; Perry, J. W.; Marder, S. R. *J. Am. Chem. Soc.* **1999**, *121*, 3715−3723.